Surface Alloying of Ti-6Al-4V with Zirconium by Pulsed Electron-Beam Melting of Film-Substrate System[1]

V.P. Rotshtein, A.B. Markov, D.I. Proskurovsky, V.A. Kagadei,
R. Guenzel *, N. Shevchenko **, H. Reuther **, V.A. Shulov ***

Institute of High-Current Electronics, 2/3 Akademichesky Ave., Tomsk, 634055, Russia,
Tel (3822)491695, Fax (3822)492410, E-mail rvp@lve.hcei.tsc.ru
** APT GmbH, Bautzner Landstr. 45, Gro?erkmannsdorf, 01454, Germany*
*** Forschungszentrum Rossendorf e. V., Institute of Ion Beam Physics and Materials Research, P.O.B. 51 01 19, Dresden, 01314, Germany*
****Moscow State Aviation Institute, 4, Volokolamskoe Sh., 125871, Moscow, Russia*

Abstract – Surface alloying of Ti-6Al-4V with Zr was realized in order to decrease in content of toxic Al and V in the surface layers and to increase in corrosion resistance. The method is based on deposition of Ti (300nm)/Zr (200 nm)/Ti (200 nm) coating on Ti-6Al-4V substrate followed by pulsed melting with a low-energy, high-current electron beam (2.5 μs, 2.5÷3 J/cm^2, 1 5 pulses). Zr-alloyed layers of thickness up to 2 m were formed and studied by SEM/EDX, AES and XRD analyses. After one-pulse alloying the near-surface layer is Zr-lean and Al-and V-reach. It consists of two Ti -based solid solutions which contain 23 and 4.5 at % Zr, respectively. Post-irradiation vacuum annealing (550 °C, 2 h) leads to substitution of Al and V by Zr in the surface layers. An increase in the number of pulses results in a decrease in Zr content near the surface and formation of cellular substructure. According to potentiodynamic tests the surface alloying provided higher corrosion resistance in 1 % NaCl solution.

1. Introduction

Titanium and titanium alloys are widely used as medical implant's materials due to a unique combination of properties (high specific strength, corrosion resistance, bio- and mechanical compatibility). During cyclic loading of implant a fretting-induced damage of thin passive TiO_2 film and the consequent release of metal ions into the surrounded tissues are occurred. In the most widely used Ti-6Al-4V alloy the greatest concern is caused with V and Al [1]. In this connection, the new surgical β-Ti alloys (Ti-13Nb-13Zr, Ti-15Zr-4Nb-4Ta, etc.), where Al and V are substituted by non-toxic alloying elements (Zr, Nb, Ta, etc.), have been developed. The biocompatibility and corrosion resistance of new alloys are noticeably higher and them mechanical properties are similar to those for Ti-6Al-4V alloy [2]. However, due to high cost their application is very limited. Simultaneously, the methods of the surface modification of Ti-6Al-4V alloy in order to increase in its corrosion resistance and biocompatibility are developed. Well-known methods (oxidation, the ion implantation, deposition of protective coatings) can't solve these problems. This is because a small thickness of the oxide and/or implanted layer, and insufficient adhesion of coatings are realized in the treated samples.

In Refs. [3–6] it has been shown, that the surface alloying of metallic materials by pulsed melting of film-substrate systems with a low-energy (~20 keV), high-current electron beam (LEHCEB) of microsecond duration is a promising method for improvement of the surface-sensitive properties.

This work is devoted to the study of the characteristics of pulsed e-beam alloying of Ti-6Al-4V with Zr. The use of the alloying for a decrease in the content of Al and V at the surface and for increase in the corrosion resistance is also of interest of the work. Zirconium was chosen because it is a biotolerant metal and its adding increases the corrosion resistance of Ti in hydrochloric, sulfuric and phosphoric acid solutions. Moreover, the complete solid solubility of two components in both α- and β-lattices takes place in Ti-Zr system [7]. The latter allows producing the surface Ti-Zr alloys at pulsed melting.

2. Experimental

The Ti and Zr films were alternately deposited onto the flat substrates of 18 mm in diameter and 3 mm thick made of Ti-6Al-4V alloy. Films were produced by magnetron sputtering (system Leibold Z-80) from a 99.9 % Ti and 99.9 % Zr disk targets of 150 mm in diameter. Prior to deposition, the substrates were mechanically polished and irradiated with a LEHCEB at the energy density E_s of 2.5÷3 J/cm^2 and pulse number N=40 in order to clean the surface of impurities [8] as well as to suppress the cratering and

[1] The work was supported by WTZ Project No. RUS 02/002

local delamination of the films under the following LEHCEB melting of film-substrate system [5]. The film-substrate system Ti (300 nm)/Zr (200 nm)/Ti (200 nm)/Ti-6Al-4V was used in experiments. The samples were irradiated with a LEHCEB at τ=2.5 μs, E_s=2.5 J/cm^2 and N=1 5. In order to decrease in residual stresses induced by pulsed e-beam heating, some of irradiated samples were annealed (550 ˚C, 2 h) in oil-free vacuum (10^{-4} Pa) [8].

The surface topography was examined with a scanning electron microscope (SEM) of Philips-SEM 515 EDAX type. The point chemical composition of the near-surface layers was determined from EDX spectra at an accelerating voltage of 30 kV. The element profiles were determined by Auger electron spectroscopy (AES) using a Microlab310F system. The phase composition of the surface layers was examined by grazing incident X-ray diffraction (GIXRD) analysis at an incident angle ω of 1÷4˚ with D5000 diffractometer as well as by X-Ray diffraction (XRD) analysis in Bregg-Brentano geometry with D8 (BRUKER AXS) diffractometer with CuK_α radiation. The thickness of an analysed layer for Ti target was 0.1÷0.8 μm for GIXRD analysis and 8÷10 μm for XRD. The corrosion behaviour was studied by potentiodynamic method (potentiostat of type AutoLab PGSTAT 12) in 1 % NaCl solution at a room temperature and potential variation rate 10 mV/s.

3. Results and discussion

3.1. Melting and crystallization

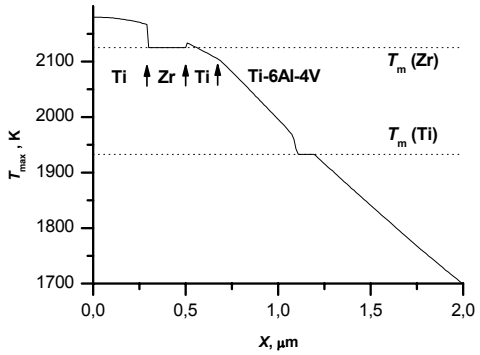

Fig .1. Calculated maximum temperature profile for Ti (300 nm)/Zr (200 nm)/Ti (200 nm)/Ti-6Al-4V system irradiated at 2.5 J/cm^2

Calculations showed that the threshold of the surface melting of Ti-6Al-4V alloy (substrate) is achieved at 2÷2.5 J/cm^2, that agrees with experiment. At E_s=2.5 J/cm^2 the thickness of the melted layer of substrate is 1.3 μm; herewith the life time of the melt is 2 μs, and the maximum crystallization front velocity and cooling rate at the melt-solid interface are 10 m/s and $5\cdot10^9$ K/s, respectively.

Fig. 1 shows the calculated maximum temperature profile for system Ti (300 nm)/Zr (200 nm)/Ti (200 nm)/Ti-6Al-4V irradiated at E_s=2.5 J/cm^2. It can be seen that both Ti layers and substrate as well are melted and total thickness of the melted layer is 1.1 μm. The life time of the melt is 3 μs. However, Zr interlayer has not melted completely, i.e. Zr exists in two-phase (solid-melt) state.

3.2. SEM/EDS observations

SEM picture of the film-substrate system surface subjected to one-pulse melting is shown in Fig. 2, *a*. The EDS point analysis shows that a two-phase Ti-Zr surface alloy is formed. It consists of the light matrix containing 23 at. % Zr and melting-off dark regions of size ranging from 1 to 15 μm containing 4.5 at. % Zr. The formation of these regions can be associated with the local overheating of Zr interlayer due to the lowered in some places local thermal contact on the Ti/Zr/Zr interfaces.

Post-irradiation annealing leads to a decrease in the sizes of dark regions and to release of Zr from these regions (up to ~1 at. % Zr) into a matrix phase (up to 26 at. % Zr). Taking into account that the low-Zr dark regions occupy about 50 % of the surface area and considering the EDS data, we can obtain the average Zr content in the near-surface layer, which appear to be 14 at. %. It should be noted, that both the local-point and the average Zr content in the near-surface layer are lower compared to the real values. This is because the thickness of EDS-investigated layer reaches some microns and exceeds the thickness of the alloyed layer. The effect of Ti-based substrate on the results of EDS measurements leads to erroneously low Zr content.

An increase in the pulse number to 5 leads to formation of the cellular substructure with an average cell size of ~10 μm (Fig. 2, *b*). The dark core of cells is similar to the dark regions formed at N=1 and contains only 2 at. % Zr. The light Zr-rich shell, in contrast, has 16 at. % Zr. On the cell boundaries, as it can be seen from contrast ratio of SEM image, the Zr content is minimal. The estimates show that for N=5 the average Zr content in the near-surface layer is about 9 at. % that is half as less than that for the one-pulse melting followed by annealing. Post-irradiation annealing leads to a small decrease in a contrast ratio of SEM image that indirectly testifies to more uniform distribution of Zr. Further experiments are needed to elucidate the formation of the cellular substructure.

3.3. AES depth profiles

As it follows from AES, as-deposited system excepting for Ti and Zr elements contains C and O impurities also. Carbon is located, mainly, in the surface layer of ~25 nm thickness, and oxygen is observed at the surface and at the film-substrate interface as well (Fig. 3, *a*).

After one-pulse melting (see Fig. 3, *b*) the mixing of elements of coating and substrate in the surface la-

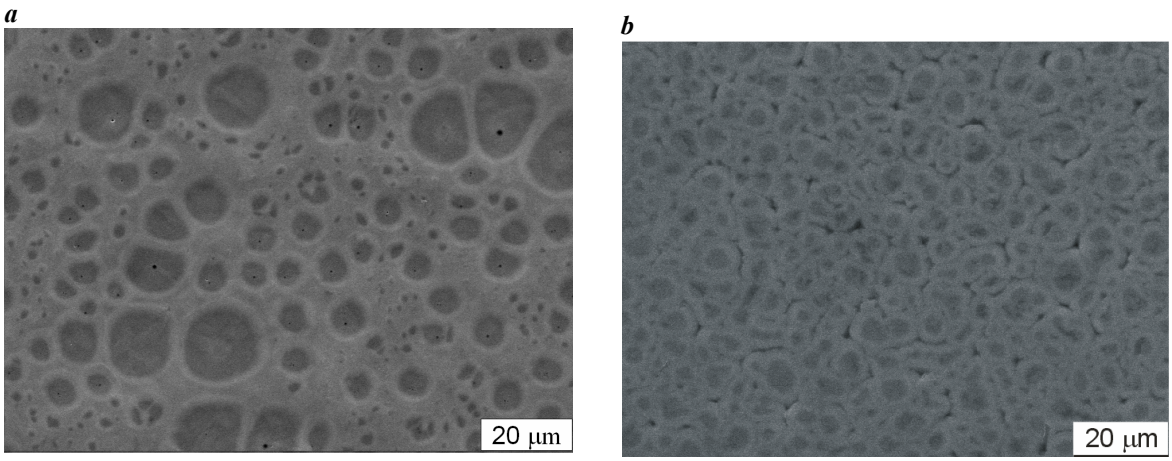

Fig. 2. SEM images of the surface of Ti (300 nm)/Zr (200 nm)/Ti (200 nm)/Ti-6Al-4V system irradiated at 2.5 J/cm^2: N=1 (a); N=5 (b)

yer of 1.5÷2 μm thickness, and a cleaning of the surface from C and O impurities as well are occurred. The near-surface layer of 300 nm thickness is enriched with Al and V but Zr is practically absent near the surface. The dipper alloyed layers contain from 10 to 20 at. % Zr.

Taking into account that a life time of the melt tm is 10^{-6} s and considering that diffusivity in the melt D equals to 5×10^{-9} m^2/s, we can receive the thickness of diffusion layer $l\sim(2D\times t_m)^{0.5}\sim100$ nm that is comparable with thickness of Ti and Zr layers. Therefore, the alloying layer was formed due to liquid-phase mixing of coating and substrate elements.

The enrichment of near-surface layers with Al and V after pulsed melting (see Fig. 3, *b*) agrees with phase diagrams of Ti-Al, Ti-V, Zr-Al and Zr-V sy-

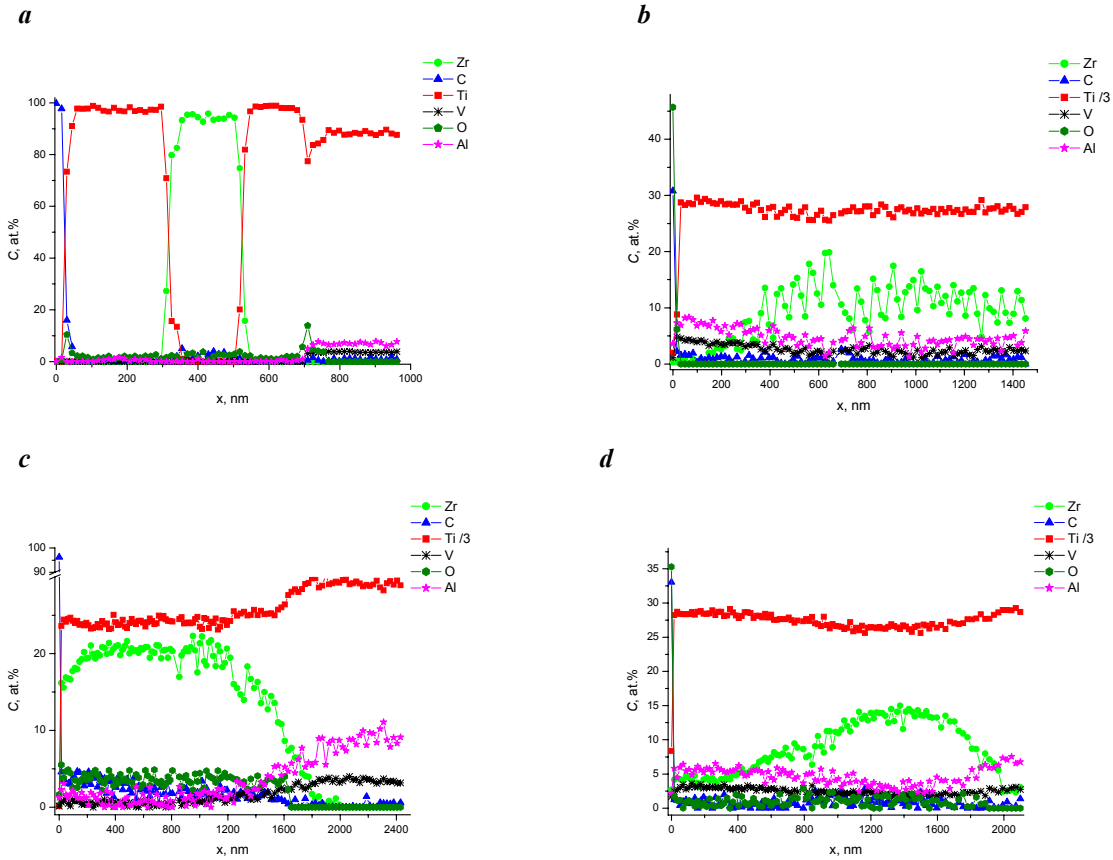

Fig. 3. Element profiles for Ti (300 nm)/Zr (200 nm)/Ti (200 nm)/Ti-6Al-4V system: as deposited (a); irradiated at 2.5 J/cm^2, N=1 (b); irradiated at 2.5 J/cm^2, N=1 followed by annealing (c); irradiated at 2.5 J/cm^2, N=5 followed by annealing (d)

stems. These systems have partition coefficient of impurity (Al and V) $K_0<1$. It means that Al and V during crystallization will be pushed out from a growing crystal and will be accumulated at the surface, as it is observed in experiment.

Post-irradiation vacuum annealing (see Fig. 3, *c*) leads, firstly, to Zr diffusion toward the surface and to more uniform Zr distribution, secondly, that is rather important, to displacement of Al and V from the surface toward the substrate. The latter results in that the alloyed layer of ~1 μm thickness contains 1.1 at. % Al and 0.5 at. % V, that is 8 and 6 times less, than that for the substrate (Ti-6Al-4V alloy) and, thirdly, to increase in O and C impurities content in the alloyed layer.

The redistribution of Zr is determined by gradients of concentration of Zr (Fig. 3, *b*). As follows from Fig. 3, *b*, *c*, the diffusion length of Zr atoms to the surface during annealing is $l \geq 200$ nm. This corresponds to diffusivity of Zr in the alloyed layer $D=3\cdot10^{-18}$ m^2/s. According to Ref. [9], the diffusivity of Zr in Ti at $T=550$ °C is $3\cdot10^{-21}$ m^2/s. Therefore, the diffusivity of Zr in the Ti-based surface alloy in our case is three orders of magnitude more than that in equilibrium conditions. Higher diffusivity of Zr can be elucidated by high concentration of quenched defects (vacancies, new inter-phase boundaries, dislocations) formed due to high-rate crystallization of the melt.

The diffusion of Al and V during annealing occurs in direction of higher concentration (toward substrate) therefore the uphill diffusion of these elements takes place. Herewith, a correlation between local peeks (falls) of Al content and falls (peeks) of Zr content is observed. It can be explained as follows. Zr unlike Al and V is dissolved completely in a solid Ti. Therefore, Zr and Ti atoms during annealing can mainly form the grains of α-(Ti,Zr) solid solution, substituting the positions Al and V in Ti lattice. The relaxation of the residual stresses in the alloyed layer during annealing [8] can stimulate this process. Al and V atoms, leaving their positions, can migrate over defects into deeper layers in direction of decrease of Zr content that will lead to decrease in Zr content in the near-surface layer.

Enrichment of alloyed layer with O and C impurities during annealing is caused by their influx from the residual gases of a vacuum chamber. The enhanced diffusivity of O and C in the target can be caused by a high concentration of quenched defects in the alloyed layer. Note that Zr, in comparison with Ti, Al and V possesses the greatest affinity to oxygen and carbon. Therefore, during annealing Zr atoms can preferentially to form dispersion second phase particles of type ZrO_2 and ZrC.

An increase in the pulse number N to 5 followed by vacuum annealing leads to an increase in the alloyed layer thickness up to 2 μm and to decrease in Zr content to 4–5 at. % at the surface layer of thickness of 500 nm (see Fig. 3, *d*). Last one is in agreement with EDS examinations. The low Zr content is accompanied by high Al and V concentration: at depth ~500 nm the surface alloy contains 5.8 at. % Al and 2.7 at. % V. Such redistribution of Zr, Al and V can be explained as follows. In case of five-shot pulsed melting the near-surface layers are enriched with Al and V more than at $N=1$, that leads to displacement of Zr into dipper layers. Therefore, at the following annealing, Zr has not enough time to distribute uniformly in depth of alloyed layer, as in case for $N=1$. Note, that even at $N=5$ a loss of Zr due to evaporation has not exceeded 10 %.

Thus, pulsed melting of a given film-substrate system followed by vacuum annealing allows to realize the surface alloying of Ti-6Al-4V with Zr at depth 1÷2 μm and herein to inhibit a release of Al and V at the surface.

3.4. Evolution of phase composition

Fig. 4 shows the XRD patterns of a given film-substrate system as deposited, after pulsed melting, and pulsed melting followed by vacuum annealing. The XRD patterns of as-deposited system (2) contain the α-Ti and α-Zr peeks. After one-pulse melting (3) the α-Zr peeks which are not overlapped with α-Ti peeks are absent, that testifies to dissolution of Zr in α-Ti lattice. Dissolution of Zr is accompanied by broadening of the Ti_α peeks and arising of new reflections which located left on the α-Ti peeks. Post-irradiation annealing (4) leads to an increase in the intensity of new reflections and to the decrease in their broadening as well as broadening of Ti_α peeks. The latter testifies to increase in the fraction of a new phase in the alloyed layer and decrease in the microstresses.

After five-shot pulsed melting followed by annealing (5), a fraction of a new phase occurred in the near-surface (0.3÷0.5 μm) layer decreases noticeably. According to AES (see Fig. 3, *d*), in this treatment mode, the Zr content at the surface dramatically decreases in comparison with one-pulse melting. From these results it follows that a new phase can be identified as a α-(Ti,Zr) solid solution.

The formation of the two-phase microstructure consisting of practically pure Ti_α and α-(Ti,Zr) solid solution agrees with SEM/EDS observations (see Sec. 3.2). In case of one-pulse melting without and with the post-irradiation annealing (see X-ray patterns 3 and 4 in Fig. 4), fractions of both phases are approximately equal each other. From these results and AES data (see Fig. 3, *b*, *c*) it follows that Zr content in a α-(Ti,Zr) solid solution is two times more than that the average value measured with AES, i.e. it is estimated to be 30÷40 at. %.

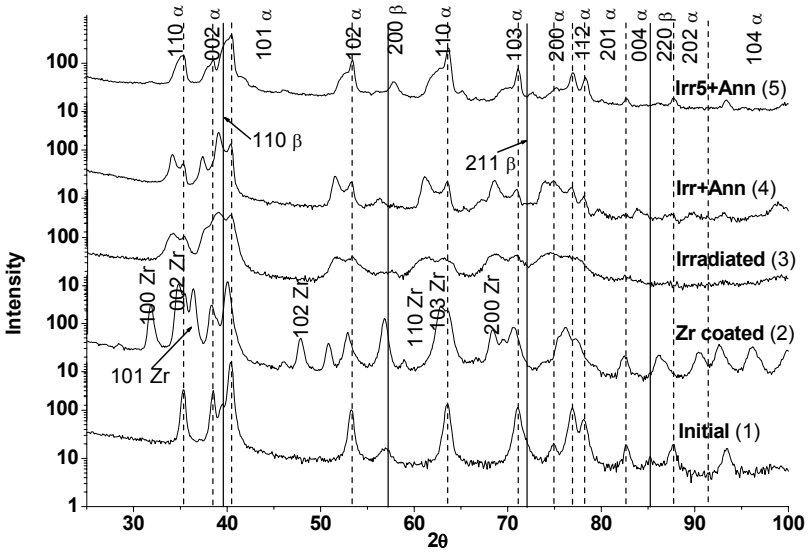

Fig. 4. GIXRD (ω=2°) patterns of the near-surface layer of Ti-6Al-4V alloy (1) and Ti (300 nm)/Zr (200 nm)/Ti (200 nm)/Ti-6Al-4V system: (2) as deposited; (3) irradiated at 2.5 J/cm^2, N=1; (4) irradiated at 2.5 J/cm^2, N=1 followed by annealing; (5) irradiated at 2.5 J/cm^2, N=5 followed by annealing. Reflections of Ti are given at the top of the figure

3.5. Corrosion behavior

Fig. 5 shows the anodic polarization curves for substrate (Ti-6Al-4V alloy, see curve1) as well as for the given film-substrate system subjected to one- and five-shot pulsed melting with and without the following vacuum annealing (see curves 2–5). As it is shown, five-shot pulsed melting leads to a noticeable (0.2 V) increase in the corrosion potential and to a decrease in the corrosion current density more than one order of magnitude compared to Ti-6Al-4V alloy. This points to an increase in the passivation and corrosion resistance of the irradiated surface. These results agree with Refs.[7, 10] where positive effect of Zr on corrosion behavior of Ti alloys was described. At N=1 the positive effect of surface alloying decreases. This agrees with SEM observations (Fig. 2) from which it follows that the microstructure formed at N=5 is more uniform than that at N=1.

Post-irradiation vacuum annealing leads to a decrease in the corrosion resistance of a surface alloy, particularly, after five-shot pulsed melting. According to GIXRD data (see Fig. 4) this could be caused by formation of the more heterogeneous two-phase microstructure after annealing.

4. Conclusions

1. Under one-pulse melting of the film-substrate system Ti (300 nm)/Zr(200 nm)/Ti (200 nm)/Ti-6Al-4V with a LEHCEB the Ti_α-based surface alloy of 1÷2 μm thickness is formed. It composed of two solid solutions containing 23 and 4.5 at. % Zr, respectively.
2. Post-irradiation vacuum annealing leads to a substitution of Al and V by Zr in the surface alloy.

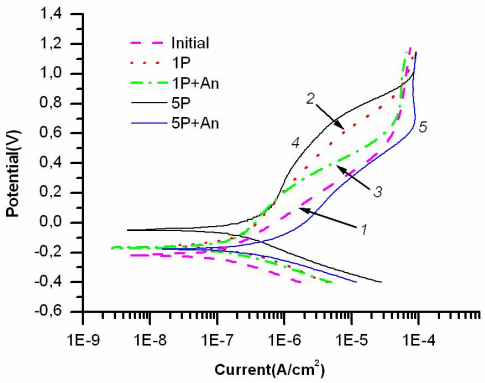

Fig. 5. Anodic polarization curves in 1 % NaCl solution for Ti-6Al-4V alloy (1) and Ti (200 nm)/Zr (100 nm)/Ti (200 nm)/alloy system: (2) irradiated at 2.5 J/cm^2, N=1 (3) irradiated at 2.5 J/cm^2, N=1 followed by annealing; (4) irradiated at 2.5 J/cm^2, N=5; (5) irradiated at 2.5 J/cm^2, N=5 followed by annealing

3. An increase in the pulse number N to 5 results in a decrease in Zr content in the near-surface layer and formation of the cellular substructure.
4. Surface alloying of Ti-6Al-4V with Zr provided higher corrosion resistance in 1 % NaCl solution.

The authors would like to thank K. Karlik for the irradiation of samples.

References

[1] S.G. Steinemann, In: *Evaluation of biomaterials.* Eds. G.D. Winter, J.L. Leray, and K. de Goot, Wiley, Chichester, 1980, pp.1–34.

[2] M. Niinomi, Metallurgical and materials transactions A 33A, 447 (2002).

[3] G.E. Ozur, D.I. Proskurovsky, V.P. Rotshtein, and A.B. Markov, Laser and Particle Beams 21, 157, (2003).

[4] V.P. Rotshtein, D.I. Proskurovsky, G.E. Ozur, Yu. F. Ivanov, A.B. Markov, Surf. Coat. Technol. 180–181, 377, (2004).

[5] V.P. Rotshtein, Yu.F. Ivanov, A.B. Markov, D.I. Proskurovsky, K.V. Karlik, K.V. Oskomov, B.V. Uglov, A.K. Kuleshov, M.V. Novitskaya, S.N. Dub, Y. Pauleau and I.A. Shulepov, Surf. Coat. Technol. 200, 6378, (2006).

[6] V. Rotshtein, Yu. Ivanov, A. Markov. In: *Materials surface processing by directed energy techniques*, Ed. by Y. Pauleau, Elsevier, 2006, pp. 205–240.

[7] U. Zwicker. *Titan und Titanlegierungen*, Springer-Verlag, Berlin, 1974.

[8] V.P. Rotshtein, R. Gunzel, A.B. Markov, D.I. Proskurovsky, M.T. Pham, E. Richter, V.A. Shulov, Rus. Fizika i Himiya Obrabotki Materialov, 1, 62, (2006).

[9] L. Pavlinov, Phys. Met. Metallogr. 24, 70, (1967).

[10] N.D. Tomashov, Rus. Zaschita metallov, 22, 865, (1986).